

## Furan Based Cyclic Oligopeptides Selectively Target G-Quadruplex

Tushar Kanti Chakraborty,<sup>\*,†</sup> Amit Arora,<sup>‡</sup> Saumya Roy,<sup>†</sup> Niti Kumar,<sup>‡</sup> and Souvik Maiti<sup>\*,†</sup>

Indian Institute of Chemical Technology, Hyderabad 500 007, India, and Proteomics and Structural Biology Unit, Institute of Genomics and Integrative Biology, Mall Road, New Delhi 110 007, India

Received May 30, 2007

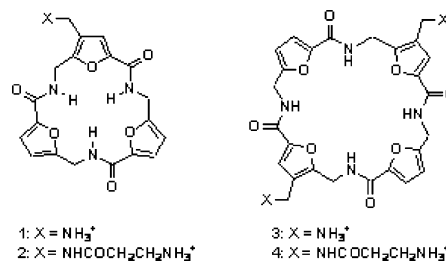
**Abstract:** We report the binding properties of 18- and 24-membered cyclic oligopeptides developed from a novel furan amino acid, 5-(aminomethyl)-2-furancarboxylic acid, to G-quadruplex. Comparative analysis of the binding data of these ligands with G-quadruplex and double-strand DNA shows that 24-membered cyclic peptides are highly selective for telomeric G-quadruplex structures and thus can be used as a scaffold to target quadruplex structures at the genomic level.

The termini of eukaryotic chromosomes are composed of specialized DNA nucleoprotein complexes termed telomeres. In mammals, telomeric DNA consists of a tandem array of the 6-nucleotide (nt) repeat 5'-TTAGGG-3'/3'-CCCTAA-5', approximately 4–14 kb long in humans, terminating in a 150–200-nt 3' single-strand DNA overhang of the G-rich strand.<sup>1–3</sup> Telomeres can structurally organize into different conformations; for instance, the G-rich single-stranded DNA can adopt an unusual four-stranded DNA structure involving G-quartets.<sup>4,5</sup> Telomerase, a ribonucleoprotein, hybridizes to G-rich overhang via its 11-base RNA template and guides the addition of six base telomeric repeats for the extension of telomeric ends to control the growth and survival of tumor cells.<sup>6</sup> Because these G-rich overhangs have the potential to form G-quadruplexes, stabilization of these structures by quadruplex selective ligands has been shown to directly inhibit telomere elongation by telomerase in vitro.<sup>7–9</sup> Ligand-induced stabilization of intramolecular G-quadruplexes has therefore become an attractive strategy for the development of anticancer drugs.

Planar molecules with building blocks that have extended  $\pi$ -delocalized systems, which favor the molecules to stack on the face of a guanine quartet, are attractive scaffolds for developing new ligands targeting G-quadruplex selectively. Positively charged substituent analogues of parent scaffolds that interact with the grooves and loops of the quadruplex and with the negatively charged phosphate backbone are necessary to enhance the selectivity. With these molecular properties, during the past decade, several ligands and scaffolds have been identified or developed that can successfully target G-quadruplex.<sup>10–17</sup>

Recently, we have developed a novel furan amino acid, 5-(aminomethyl)-2-furancarboxylic acid, and prepared its trimer, an 18-member cyclic oligopeptide, which displayed a near-planar geometry with *s-cis* orientation of all the amide carbonyls.<sup>18</sup> The planarity of these molecules along with their aromatic rings having cationic side chains was envisaged to be ideally suited to target G-quadruplex. We report here the synthesis and the binding abilities of two cationic analogues

**Scheme 1.** Chemical Structures of Cyclic Oligomers of Furan Amino Acids 1–4



each of 18- (**1** and **2**) and 24-membered (**3** and **4**) cyclic oligopeptides of furan amino acid (Scheme 1).

The syntheses of the cyclic peptides **1–4** are given in detail in the Supporting Information. The two building blocks used are the furan amino acids H-Faa-OH and its substituted congener H-Faa(CH<sub>2</sub>N<sub>3</sub>)-OH. While the former was prepared following the reported procedure,<sup>18</sup> synthesis of the latter is described in the Supporting Information. The peptides were synthesized following standard solution-phase peptide coupling methods<sup>19</sup> using 1-ethyl-3-(3-(dimethylamino)propyl)carbodiimide hydrochloride (EDCI) and 1-hydroxybenzotriazole (HOBt) as coupling agents and dry DMF and/or CH<sub>2</sub>Cl<sub>2</sub> as solvents. The C- and N-termini were protected as the methyl ester and Boc, respectively. Saponification of the methyl esters was carried out using LiOH in THF–MeOH–H<sub>2</sub>O, and Boc deprotection of the N-termini was done using TFA in CH<sub>2</sub>Cl<sub>2</sub>. Following the fragment condensation strategy, the linear trimer was prepared and deprotected at both ends. The resulting deprotected trimer, TFA·H-Faa-Faa(CH<sub>2</sub>N<sub>3</sub>)-Faa-OH, was cyclized using pentafuorophenyl diphenylphosphinate (FDPP)<sup>20</sup> in CH<sub>3</sub>CN under dilute conditions to give the desired cyclic product cyclo-[Faa-Faa(CH<sub>2</sub>N<sub>3</sub>)-Faa] in 60% yield.

The deprotected dimer, TFA·H-Faa(CH<sub>2</sub>N<sub>3</sub>)-Faa-OH, under the same reaction conditions underwent a facile cyclodimerization to give the cyclic tetramer cyclo-[Faa(CH<sub>2</sub>N<sub>3</sub>)-Faa]<sub>2</sub> in 54% yield. The cyclized products were reduced by catalytic hydrogenation in a short reaction time to avoid any over-reduction of the furan rings, followed by in situ treatment with Boc<sub>2</sub>O to convert the azido groups into NHBoc. The products were purified at the Boc-protected stage by standard silica gel column chromatography. Then Boc deprotection using TFA–CH<sub>2</sub>Cl<sub>2</sub> provided ligands **1** and **3**. Couplings of **1** and **3** with Boc- $\beta$ -Ala-OH were again followed by Boc deprotection to provide the other two products **2** and **4**, respectively. The final products were fully characterized by spectroscopic methods before using them in the binding studies (see Supporting Information).

To obtain quantitative binding knowledge, surface plasmon resonance (SPR) studies were performed. SPR not only provides direct information about the binding of the ligands to quadruplex but also enables comparison of the binding affinity of these ligands with that obtained for DNA duplex, which is a measure of selective G-quadruplex interaction. The experiments were performed using two different immobilized DNA targets: quadruplexes formed by the human telomeric region [d(AGGG-[TTAGGG]<sub>3</sub>)] and a hairpin of a 10-mer double-strand stem of mixed base content. The binding isotherms are shown in Figure 1, and data are tabulated in Table 1. As shown in Figure 1, all the ligands bind to the quadruplex with a dissociation constant

\* To whom correspondence should be addressed. For T.K.C.: phone, +914027193154; fax, +914027193108; e-mail, chakraborty@iict.res.in. For S.M.: phone, +911127666156; fax, +9127667471; e-mail, souvik@igib.res.in.

<sup>†</sup> Indian Institute of Chemical Technology.

<sup>‡</sup> Institute of Genomics and Integrative Biology.

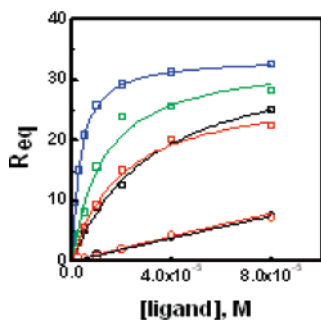


**Figure 1.** SPR binding curves for **1** (black box), **2** (red box), **3** (green box), and **4** (blue box) to telomeric quadruplex and for **1** (black circle) and **2** (red circle) to DNA hairpin in 10 mM HEPES, pH 7.4, 100 mM KCl.

**Table 1.** Dissociation Constants  $K_D$  ( $\mu\text{M}$ ) Determined by SPR and Differential Melting Temperature  $\Delta T_M$  ( $^\circ\text{C}$ ) Determined by FRET and DSC

parameter	DNA	<b>1</b>	<b>2</b>	<b>3</b>	<b>4</b>
$K_D^a$	telo	29.0	21.0	14.5	3.1
	hairpin	950	700	nd	nd
$\Delta T_M^b$	telo	9.0	10.0	12.0	17.0
	telo in presence competitor	7.0	7.0	12.0	17.0
$\Delta T_M^c$	telo	2.0	3.0	6.6	9.2

<sup>a</sup>  $K_D$  values are within 5%, and  $\Delta T_M$  values are within 0.5  $^\circ\text{C}$ . nd: none detected. <sup>b</sup> From FRET experiments. <sup>c</sup> From DSC experiments.

in the range 3–30  $\mu\text{M}$ . Though ligands **1** and **2** show binding to duplex with dissociation constants in the range 700–950  $\mu\text{M}$ , no detectable binding was noticed in the cases of **3** and **4**. This result demonstrates that 24-membered cyclic oligopeptides have higher binding affinity and selectivity for quadruplex. The higher binding affinity and selectivity of the 24-membered compound over 18-membered is most probably due to the increased ability of the tetrameric moiety to stack on the face of a guanine quartet. Of the two types of side chains used in this study, ligands **2** and **4** with amino acid side chain show lower dissociation constants than ligands **1** and **3**, respectively, with methylamino side chain. This result implies that a ligand with a longer side chain with an amino group at the end makes superior electrostatic and van der Waals interactions with the groove cavity of quadruplex compared to the ligand with a methylamino group.

Next we monitored the melting temperature of fluorescent-tagged G-quadruplexes labeled by 5'-FAM and 3'-TAMRA (5'-FAM-d(AGGG[TTAGGG]<sub>3</sub>)-TAMRA-3') representing the human telomeric (0.1  $\mu\text{M}$ ) in the presence of 1  $\mu\text{M}$  ligands (Figure 2a) in 100 mM KCl buffer. In all the cases, considerable stabilization effects were observed (Table 1) and the highest stabilization ( $\Delta T_M = 17^\circ\text{C}$ ) was observed in the case of **4**, which showed the most effective binding in the SPR experiment. The observed stabilization effects in potassium buffer at 1  $\mu\text{M}$  ligands were then challenged by the addition of a double-stranded competitor (Supporting Information, Figure 2). Addition of 500-fold molar excess (in base pairs over base quartets) of a self-complementary 20 bp dsDNA of mixed base content had very little effect on the observed stabilization. As for example with **4**, which showed the lowest dissociation constant and the highest stabilization effects, the stabilization was 17  $^\circ\text{C}$  in the case of the telomeric quadruplex in the presence of excess duplex. These results are in agreement with the SPR measurements, which indicate a preferential interaction of these ligands with the quadruplex-forming oligonucleotides.

The origin of the extra stability of the quadruplexes in the presence of different ligands was finally studied by differential scanning calorimetry (DSC). DSC measures direct heat change

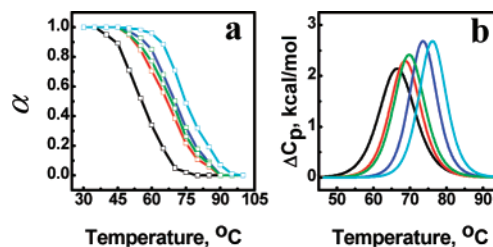


**Figure 2.** (a) FRET melting and (b) DSC trace for free quadruplex (black) and those in presence of **1** (red), **2** (green), **3** (blue), and **4** (cyan).

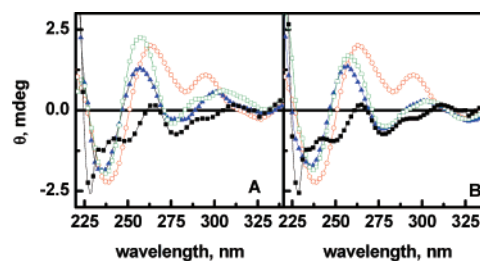


**Figure 3.** CD spectra of telomeric [d(AGGG[TTAGGG]<sub>3</sub>)] oligonucleotides (5  $\mu\text{M}$ ) in 10 mM Tris buffer in the absence of KCl (black), presence of 100 mM KCl (red), presence of 5  $\mu\text{M}$  (blue) and 10  $\mu\text{M}$  (green) of ligand **3** (A) and ligand **4** (B).

that is associated with the quadruplex (25  $\mu\text{M}$ ) melting in the absence and presence of stoichiometric amounts of ligand (1:4 quadruplex to ligand molar ratio). Figure 2b shows excess heat capacity change as a function of temperature of 25  $\mu\text{M}$  telomeric quadruplex in 100 mM KCl buffer in the presence of 100  $\mu\text{M}$  different ligand molecules. In the presence of all the ligands, telomeric quadruplex melts at higher temperatures. But the extent of enhanced thermal stability of the quadruplex in the presence of a stoichiometric amount of ligands is lower than that observed in the FRET study where ligand concentration was 10 times more than the quadruplex concentration. Enthalpy changes ( $\Delta H$ ) for the formation of telomeric quadruplex in 100 mM KCl obtained from DSC are exothermic (−32.0 kcal/mol) but are more exothermic in nature in the presence of ligands under the same conditions. The observed  $\Delta H$  was −35 kcal/mol for **1** and **2**, −38 kcal/mol for **3**, and −40 kcal/mol for **4**. These results show that binding of these ligands to quadruplex reinforces the base-pair stacking interactions of quartets, revealing that the furan rings of these cyclic peptides favor their stacking on the face of a guanine quartet.

We performed CD experiments to investigate induction of structural and conformational changes in telomeric quadruplex upon interaction with cyclic oligopeptides. We collected the CD spectrum for telomeric quadruplex in the presence of different concentrations of ligands **3** and **4** in 10 mM Tris buffer, pH 7.4, in the absence and presence of KCl because these two ligands selectively bind with quadruplex. The sequence [d(AGGG[TTAGGG]<sub>3</sub>)] adopts both parallel and antiparallel mixed conformation in the presence of 100 mM KCl with predominant positive peak at 262 nm, a small peak positive at 292 nm, and a negative peak at 240 nm.<sup>21</sup> We observed that this sequence lacks the quadruplex signature in the absence of KCl. Interestingly, upon addition of increasing concentrations of ligands **3** and **4**, we observed an increase in the parallel G-quadruplex signature (Figure 3), thus suggesting the quadruplex inducing ability of these cyclic oligopeptides. Similar results were reported recently.<sup>13,22</sup> However, ligands **3** and **4** could not induce

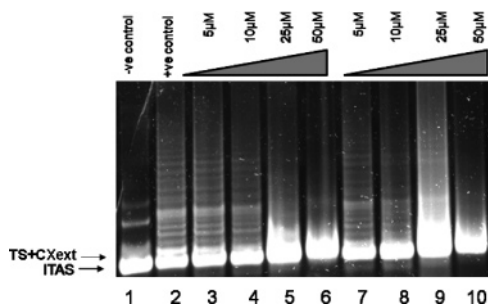


**Figure 4.** Inhibition of telomerase extension activity by PCR based TRAP assay: (lane 1) –ve control, TRAP without telomerase extract; (lane 2) +ve control, telomerase extract with no added ligands; (lanes 3–6) ligand **3**; (lanes 7–10) ligand **4**. Inhibition of telomeric ladder started at 25  $\mu\text{M}$  (lanes 5, 9) for ligands **3** and **4** and is achievable at 50  $\mu\text{M}$  (lanes 6, 10). TS+CXext is the minimal dimer representing telomerase activity. ITAS represents internal control.

any conformational changes in the telomeric quadruplex structure in the presence of 100 mM KCl.

The promising biophysical results prompted us to perform biological assays for these ligands. We carried out MTT assay to check the cytotoxicity of the ligands in A549 cells. The  $\text{IC}_{50}$  values obtained from the MTT assay were found to be 500  $\mu\text{M}$  for ligands **3** and **4** (Supporting Information, Figure 3). They were found to be considerably less toxic compared to the other well-studied ligands. Low cytotoxicity of these ligands raises the issue of cellular uptake. Direct evidence demonstrating cellular uptake would involve tagging the ligand with a fluorescent probe and observing its localization through fluorescence microscopy. However, attachment of a fluorescent tag to ligands **3** and **4** would affect the entire physical chemistry of interaction. We performed cell cycle analysis,<sup>23</sup> which would provide the effect of the ligands on cell cycle progression in different phases of growth and hence provide indirect evidence of cellular uptake. Cell cycle study shows an increase in the population of cells in the G1 phase (growth phase) of cell cycle upon treatment with ligand **3** and **4** in comparison to the control (untreated cells, Supporting Information Figure 5). This observation clearly indicates the cellular uptake of these ligands.

Next we performed the PCR based telomeric repeat amplification protocol (TRAP) assay, which was followed by photometric enzyme immunoassay for the detection of telomerase activity.<sup>24</sup> G-quadruplex interactive agents block telomerase activity through the stabilization of G-quadruplex structures, prevent the primer from binding to the hTR RNA template of telomerase, and hamper its extension. We performed PCR based TRAP at different concentrations of ligand and observed inhibition of the characteristic telomeric ladder suggestive of inhibition of telomere extension and telomerase activity. The ligands used in the study stabilize the quadruplex structure as observed in fluorescence and DSC studies and prevent the telomerase activity leading to the disappearance of the characteristic ladder (Figure 4). Internal control (ITAS), a 36 bp product, allows discrimination between telomerase inhibition and Taq polymerase inhibition. Figure 4 shows no inhibition of ITAS, indicating no polymerase inhibition by ligands **3** and **4**. An ELISA based TRAP assay was carried out to quantify the telomerase activity in the presence of increasing concentrations of ligands **3** and **4**. The data quantified from this assay are in concordance with the data presented in Figure 4. The relative units of TRAP activity are found to be maximum for positive and minimum for negative control, respectively, as shown in Supporting Information, Figure 5. Quadruplex interacting ligands display dose-dependent inhibition of the telomere

ladder. However, higher ligand concentrations can lead to non-G-quadruplex mediated effects involving inhibition of telomerase, primer dimerization, or PCR amplification through Taq polymerase inhibition.<sup>24</sup> Our data suggest that both ligands inhibit telomerase activity considerably by stabilizing G-quadruplex structure, but higher ligand concentrations produce non-G-quadruplex related telomerase inhibition. Similar results were also reported in the literature.<sup>24</sup>

Recently, Jantos et al. have reported binding properties of oxazole-based peptide macrocycles with the c-kit and human telomeric quadruplex.<sup>17</sup> The structural diversity between the above-mentioned reported molecules and the ligands studied here is not only the different building blocks (oxazole vs furan) used to build the molecules but also the placement and the chemistry of the side chains. Placing the side chains on the heterocyclic rings rather than on the carbon atom adjacent to amino groups makes the synthesis easier and will not affect the planarity of the molecules. In spite of having such diversity, newly synthesized molecules have similar binding affinities as reported for the oxazole-based peptide macrocycles. The toxicity and biological activities of the oxazole-based peptide macrocycles have not been reported and thus cannot be compared with ligands reported in the current study. But the reported thermodynamic preference of the oxazole-based peptide macrocycles for binding to a parallel G-quadruplex structure (c-kit quadruplex) compared to an antiparallel conformation (human telomeric quadruplex) is worth testing for the molecules studied here, and work is in progress.

In conclusion, we show that 18- and 24-membered cyclic oligopeptides developed from a novel furan amino acid, 5-(aminomethyl)-2-furancarboxylic acid, having one and two cationic side chains are able to interact with G-quadruplex structures selectively and thus stabilize the structures. These ligands have low cytotoxicity and are able to efficiently inhibit the activity of telomerase, which makes them promising ligands for exploration for anticancer therapy.

**Acknowledgment.** We thank CSIR and DST, New Delhi, for financial support and CSIR (S.R., N.K.) and UGC (A.A.), New Delhi, for research fellowships.

**Supporting Information Available:** Experimental section, NMR, mass and elemental analysis data, and cell cycle analysis. This material is available free of charge via the Internet at <http://pubs.acs.org>.

## References

- Wright, W. E.; Tesmer, V. M.; Huffman, K. E.; Levene, S. D.; Shay, J. W. Normal human chromosomes have long G-rich telomeric overhangs at one end. *Genes Dev.* **1997**, *11*, 2801–2809.
- McElligott, R.; Wellinger, R. J. The terminal DNA structure of mammalian chromosomes. *EMBO J.* **1997**, *16*, 3705–3714.
- Makarov, V. L.; Hirose, Y.; Langmore, J. P. Long G tails at both ends of human chromosomes suggest a C strand degradation mechanism for telomere shortening. *Cell* **1997**, *88*, 657–666.
- Parkinson, G. N.; Lee, M. P.; Neidle, S. Crystal structure of parallel quadruplexes from human telomeric DNA. *Nature* **2002**, *417*, 876–880.
- Schaffitzel, C.; Berger, I.; Postberg, J.; Hanes, J.; Lipps, H. J.; Plückthun, A. In vitro generated antibodies specific for telomeric guanine-quadruplex DNA react with *Stylynychia lemnae* macronuclei. *Proc. Natl. Acad. Sci. U.S.A.* **2001**, *98*, 8572–8577.
- Bodnar, A. G.; Ouellette, M.; Frolkis, M.; Holt, S. E.; Chiu, C. P.; Morin, G. B.; Harley, C. B.; Shay, J. W.; Lichtsteiner, S.; Wright, W. E. Extension of life-span by introduction of telomerase into normal human cells. *Science* **1998**, *279*, 349–352.
- Zahler, M.; Williamson, J. R.; Cech, T. R.; Prescott, D. M. Inhibition of telomerase by G-quartet DNA structures. *Nature* **1991**, *350*, 718–720.
- Shammas, M. A.; Shmookler Reis, R. J.; Akiyama, M.; Koley, H.; Chauhan, D.; Hideshima, T.; Goyal, R. K.; Hurley, L. H.; Anderson, K. C.; Munshi, N. C. *Mol. Cancer Ther.* **2003**, *2*, 825–833.

- (9) Tahara, H.; Shin-ya, K.; Seimiya, H.; Yamada, H.; Tsuruo, T.; Ide, I. G-Quadruplex stabilization by telomestatin induces TRF2 protein dissociation from telomeres and anaphase bridge formation accompanied by loss of the 3' telomeric overhang in cancer cells. *Oncogene* **2006**, *25*, 1955–1966.
- (10) Baker, E. S.; Lee, J. T.; Sessler, J. L.; Bowers, M. T. Cyclo[n]pyrroles: size and site-specific binding to G-quadruplexes. *J. Am. Chem. Soc.* **2006**, *128*, 2641–2648.
- (11) Reed, J. E.; Arnal, A. A.; Neidle, S.; Vilar, R. Stabilization of G-quadruplex DNA and inhibition of telomerase activity by square-planar nickel(II) complexes. *J. Am. Chem. Soc.* **2006**, *128*, 5992–5993.
- (12) Seenisamy, J.; Bashyam, S.; Gokhale, V.; Vankayalapati, H.; Sun, D.; Siddiqui-Jain, A.; Streiner, N.; Shin-ya, K.; White, E.; Wilson, W. D.; Hurley, L. H. Telomestatin and diseleno saphyrin bind selectively to two different forms of the human telomeric G-quadruplex structure. *J. Am. Chem. Soc.* **2005**, *127*, 2944–2959.
- (13) Rodriguez, R.; Pantos, G. D.; Goncalves, D. P.; Sanders, J. K.; Balasubramanian, S. Ligand-driven G-quadruplex conformational switching by using an unusual mode of interaction. *Angew. Chem., Int. Ed.* **2007**, *46*, 5405–5407.
- (14) Teulade-Fichou, M.-P.; Carrasco, C.; Guittat, L.; Bailly, C.; Alberti, P.; Mergny, J.-L.; David, A.; Lehn, J.-M.; Wilson, W. D. Selective recognition of G-quadruplex telomeric DNA by a bis(quinacridine) macrocycle. *J. Am. Chem. Soc.* **2003**, *125*, 4732–4740.
- (15) Schouten, J. A.; Ladame, S.; Mason, S. J.; Cooper, M. A.; Balasubramanian, S. G-quadruplex-specific peptide–hemicyanine ligands by partial combinatorial selection. *J. Am. Chem. Soc.* **2003**, *125*, 5594–5595.
- (16) Kim, M. Y.; Vankayalapati, H.; Shin-ya, K.; Wierzbka, K.; Hurley, L. H. Telomestatin, a potent telomerase inhibitor that interacts quite specifically with the human telomeric intramolecular G-quadruplex. *J. Am. Chem. Soc.* **2002**, *124*, 2098–2099.
- (17) Jantos, K.; Rodriguez, R.; Ladame, S.; Shirude, P. S.; Balasubramanian, S. Oxazole-based peptide macrocycles: a new class of G-quadruplex binding ligands. *J. Am. Chem. Soc.* **2006**, *128*, 13662–13663.
- (18) (a) Chakraborty, T. K.; Tapadar, S.; Kumar, S. K. Cyclic trimer of 5-(aminomethyl)-2-furancarboxylic acid as a novel synthetic receptor for carboxylate recognition. *Tetrahedron Lett.* **2002**, *43*, 1317–1320. (b) Chakraborty, T. K.; Tapadar, S.; Raju, T. V.; Annapurna, J.; Singh, H. Cyclic trimers of chiral furan amino acids. *Synlett* **2004**, 2484–2488.
- (19) (a) Bodanszky, M.; Bodanszky, A. *The Practices of Peptide Synthesis*; Springer-Verlag: New York, 1984. (b) Grant, G. A. *Synthetic Peptides: A User's Guide*; W. H. Freeman: New York, 1992. (c) Bodanszky, M. *Peptide Chemistry: A Practical Textbook*; Springer-Verlag: Berlin, 1993.
- (20) (a) Leonard, M. S.; Joullie, M. M. *Encyclopedia of Reagents for Organic Synthesis*; John Wiley & Sons, Ltd.: New York, 2002. (b) Bertram, A.; Hannam, J. S.; Jolliffe, K. A.; de Turiso, F. G. L.; Pattenden, G. The synthesis of novel thiazole containing cyclic peptides via cyclooligomerisation reactions. *Synlett* **1999**, 1723–1726.
- (21) Dai, J.; PUNCHIHewa, C.; Ambrus, A.; Chen, D.; Jones, R. A.; Yang, D. Structure of the intramolecular human telomeric G-quadruplex in potassium solution: a novel adenine triple formation. *Nucleic Acids Res.* **2006**, *35*, 2440–2450.
- (22) Fu, B.; Huang, J.; Ren, L.; Weng, X.; Zhou, Y.; Du, Y.; Wu, X.; Zhou, X.; Yang, G. Cationic corrole derivatives: a new family of G-quadruplex inducing and stabilizing ligands. *Chem. Commun.* **2007**, *31*, 3264–3266.
- (23) Lodish, H.; Berk, A.; Zipursky, S. L.; Matsudaira, P.; Baltimore, D.; Darnell, J. E. *Molecular Cell Biology*; W. H. Freeman & Co.: New York, 2000.
- (24) Gomez, D.; Mergny, J. L.; Riou, J. F. Detection of telomerase inhibitors based on G-quadruplex ligands by a modified telomeric repeat amplification protocol assay. *Cancer Res.* **2002**, *62*, 3365–3368.

JM070619C